

Magnetoresistance of Oriented Gray Tin Single Crystals*

O. N. TUFTET† AND A. W. EWALD

Department of Physics, Northwestern University, Evanston, Illinois

(Received September 16, 1960)

The electronic band structure of gray tin was investigated through magnetoresistance measurements on oriented *n*- and *p*-type single crystals at 77, 195, and 273°K. From these measurements the low-field magnetoresistance coefficients were evaluated. Magnetoresistance anisotropy was observed in *n*-type crystals at 195 and 273°K, but was not observed in either *n*- or *p*-type material at 77°K. Two possible explanations for the temperature-dependent anisotropy are proposed. The observed anisotropy satisfies, within the experimental uncertainty, the symmetry condition for ellipsoidal energy surfaces located along the [111] directions. Hall and conductivity measurements on samples used in the magnetoresistance study revealed a temperature-dependent mobility ratio greater than unity which supports the assumption that the magnetoresistance anisotropy observed in the intrinsic range should be assigned to the conduction band. Under this assumption and that of isotropy of lattice scattering, a lower limit of 2.3 is found for the electronic effective-mass anisotropy parameter.

I. INTRODUCTION

THE availability of gray tin single crystals¹ enables one, by means of magnetoresistance measurements on oriented samples, to obtain experimental information on the energy band structure of this semiconductor. The relation between the phenomenological magnetoresistance coefficients^{2,3} and the energy band structure for cubic semiconductors has been well established by extensive work on germanium and silicon.⁴ For gray tin, however, previous magnetoresistance measurements,⁵⁻⁸ because they were all made on polycrystalline specimens, did not yield the coefficients required for a similar analysis.

The present paper reports magnetoresistance measurements on oriented specimens of gray tin. Measurements of the longitudinal and transverse magnetoresistance as a function of crystal orientation and magnetic field strength were made on *n*-type samples at 77°, 195°, and 273°K and on a *p*-type sample at 77°K. The phenomenological coefficients were evaluated at each temperature and, using the results of magnetoresistance calculations for ellipsoidal surfaces of constant energy in *k* space,⁹⁻¹² the effective mass anisotropy was estimated.

II. SPECIMEN PREPARATION AND EXPERIMENTAL PROCEDURE

The single crystals of gray tin used in this work were grown from mercury solution¹ using Vulcan tin of 99.999% purity. Crystals grown at -25°C or below are always *n* type due to the presence of *n*-type impurities in the original tin. At these temperatures, the solubility of mercury in gray tin is sufficiently low that the *p*-type conductivity resulting from mercury in solid solution is negligible. All *n*-type crystals used in this study were grown under these conditions and had carrier concentrations of approximately 10^{17}cm^{-3} . The *p*-type crystals were grown from a solution doped with indium. Samples in the form of rectangular parallelepipeds having dimensions of the order of 5 mm×0.5 mm×0.3 mm were cut from the crystals with an "Airbrasive" sandblast unit. During cutting the crystal was cooled with liquid nitrogen to prevent transformation to the metallic phase. The long dimension of each sample coincided with either the [100] or [110] crystallographic axis, and one of the smaller dimensions was along the [001] axis. Sample orientation was verified by Laue patterns to be within 2° of the specified direction.

The sample holder was provided with current electrodes and four potential probes for conductivity and Hall effect measurements. The current electrodes consisted of 1-mil thick copper foil and the potential probes were 1.5-mil copper wire. The electrodes were soldered to the sample with a 23% indium-77% gallium alloy having a melting point of 16°C. The current electrode solder spots covered the entire ends of the crystal while the probe spots were kept as small as possible, usually about 0.1 mm in diameter. The sample length-to-width ratio was sufficient in all cases that negligible shorting of the Hall voltage by the current electrodes occurred.¹³ For some *n*-type samples, the extra probes for Hall measurements were attached after the magnetoresistance measurements had been completed.

* This work was supported by the Office of Naval Research. It is based upon the thesis submitted by one of the authors (O. N. T.) to the Graduate School of Northwestern University in partial fulfillment of the requirements for the Ph.D. degree.

† Present address: Honeywell Research Center, Hopkins, Minnesota.

¹ A. W. Ewald and O. N. Tufte, *J. Appl. Phys.* **29**, 1007 (1958).

² F. Seitz, *Phys. Rev.* **79**, 372 (1950).

³ G. L. Pearson and H. Suhl, *Phys. Rev.* **83**, 768 (1951).

⁴ See for example the review article by M. Glicksman in *Progress in Semiconductors* (John Wiley & Sons, Inc., New York, 1958), Vol. 3, p. 1.

⁵ G. Busch and J. Wieland, *Helv. Phys. Acta* **26**, 697 (1953).

⁶ J. T. Kendall, *Phil. Mag.* **45**, 141 (1954).

⁷ A. W. Ewald and E. E. Kohnke, *Phys. Rev.* **97**, 607 (1955).

⁸ J. H. Becker, thesis, Cornell University, Ithaca, New York, 1957, (unpublished).

⁹ B. Abeles and S. Meiboom, *Phys. Rev.* **95**, 31 (1954).

¹⁰ M. Shibuya, *Phys. Rev.* **95**, 1385 (1954).

¹¹ C. Herring, *Bell System Tech. J.* **34**, 237 (1955).

¹² C. Herring and E. Vogt, *Phys. Rev.* **101**, 944 (1956).

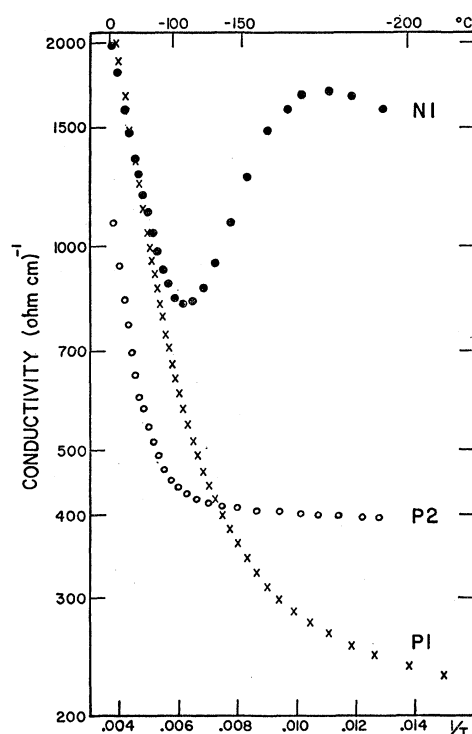
¹³ I. Isenberg, B. R. Russell, and R. F. Greene, *Rev. Sci. Instr.* **19**, 685 (1948); J. Volger, *Phys. Rev.* **79**, 1923 (1950).

TABLE I. Characteristics of gray tin samples used in the magnetoresistance study.

Sample	$T=273^\circ\text{K}$		$T=77^\circ\text{K}$			Carriers per cc
	σ_0 (ohm ⁻¹ cm ⁻¹)	R_0 (cm ² /coul)	σ_0 (ohm ⁻¹ cm ⁻¹)	R_0 (cm ² /coul)	$R_0\sigma_0$ (cm ² /v-sec)	
N1	2080		1600	-61	0.97×10^5	1.02×10^{17}
N2	2640		2000	-72	1.44×10^5	0.87×10^{17}
N3	2340	-0.232	1800	-70	1.26×10^5	0.89×10^{17}
N4	2310	-0.212	1790	-72	1.31×10^5	0.87×10^{17}
N5	2300		1710	-83	1.45×10^5	0.75×10^{17}
N6	2460	-0.215	1820	-90	1.60×10^5	0.69×10^{17}
N7	2160		1815	-78	1.40×10^5	0.80×10^{17}
N8	2310	-0.226	1810	-78	1.40×10^5	0.80×10^{17}
P1	2300		230 ^a	+6.9 ^a	1.6×10^{3a}	9.1×10^{17} ^a
P2	1210		400	+1.1	4.4×10^2	5.7×10^{18}

^a At 67°K.

A constant current, dc potentiometric method was used for all voltage measurements. Sample currents in the range from 10-50 ma were used. A Weiss-type electromagnet provided magnetic fields up to 12 kgauss. All measurements were made with the sample in a liquid bath, thus eliminating thermal effects. Constant-temperature baths having temperatures of 77°, 195°, and 273°K made use of the normal boiling point of nitrogen, the normal sublimation temperature of carbon dioxide, and the normal boiling point of butane, respectively. On using liquid propane and liquid butane, a continuous range in temperature from 83-273°K was obtained. All temperatures were measured with a copper-constantan thermocouple.

FIG. 1. Conductivity of a typical *n*-type sample and two indium-doped *p*-type samples.

III. SPECIMEN CHARACTERISTICS

The temperature dependence of the conductivity of a typical *n*-type sample and of two *p*-type samples is shown in Fig. 1. Hall curves for the same samples are shown in Fig. 2. In Table I values of the conductivity and Hall coefficient at 77° and 273°K are tabulated together with $R_0\sigma_0$ products and carrier concentrations. The values of the zero-field Hall coefficient R_0 were obtained by extrapolation. The carrier concentrations were calculated from the low-temperature Hall coefficients assuming degeneracy. Since all samples but P2 are not quite extrinsic at the lowest measurement temperature, the calculated values are presumed to be generally higher than the actual impurity concentrations.

An interesting conclusion to be drawn from the *p*-type curves is that the mobility ratio b is temperature dependent. For sample P1, which shows a Hall crossover at 94°K, the maximum (negative) Hall coefficient is significantly greater in absolute value than the Hall coefficient in the exhaustion region, whereas the reverse is true for sample P2 which crosses over at 230°K. Application of the method of Breckenridge *et al.*¹⁴ yields mobility ratios of 6.0 at 133°K and 2.0 at 278°K; these temperatures are the positions of the maxima for P1 and P2, respectively.¹⁵ The mobility ratio at an intermediate temperature can be evaluated by applying Hunter's method¹⁶ to the conductivity curve of sample P2. This yields the value 3.3 at 192°K. The three values of b are consistent with a $T^{-3/2}$ temperature dependence and are larger than most previous determinations of the mobility ratio,^{5,17} although some measurements of Becker⁸ yielded a ratio of 10 at 100°K.

¹⁴ R. G. Breckenridge, R. F. Blunt, W. R. Hosler, H. P. R. Fredrickse, J. H. Becker, and W. Oshinsky, Phys. Rev. **96**, 571 (1954).

¹⁵ The values of b are assigned to the temperatures of the Hall maxima because the exhaustion Hall coefficient is independent of b . The location of the maximum of P2 involves a slight extrapolation. In applying this method we assume that the temperature dependence of b is weak in comparison with that of the minority carrier density.

¹⁶ L. P. Hunter, Phys. Rev. **91**, 579 (1953).

¹⁷ A. N. Goland and A. W. Ewald, Phys. Rev. **104**, 948 (1956).

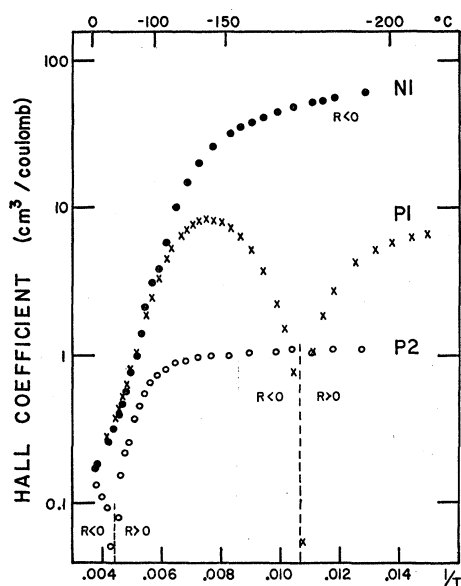


FIG. 2. Hall coefficient of a typical n -type sample and two p -type samples.

IV. EVALUATION OF THE PHENOMENOLOGICAL MAGNETORESISTANCE COEFFICIENTS

The phenomenological equation relating the electric field \mathbf{E} and current density \mathbf{J} in cubic crystals is^{2,3}

$$\mathbf{E} = \rho_0[\mathbf{J} + A(\mathbf{J} \times \mathbf{H}) + B\mathbf{J}H^2 + C\mathbf{H}(\mathbf{J} \cdot \mathbf{H}) + D\mathbf{T}\mathbf{J}], \quad (1)$$

where T is a diagonal tensor having components H_1^2 , H_2^2 , and H_3^2 in a coordinate system (1,2,3) coinciding with the cubic crystal axes, ρ_0 is the electrical resistivity, A is the Hall coefficient, and B , C , and D are the phenomenological magnetoresistance coefficients. Terms involving the magnetic field to greater than the second power are neglected in this equation. If $\mu H \ll 10^8$, the relation between the magnetoresistance and the phenomenological coefficients is³

$$\Delta\rho/\rho_0 H^2 = B + C(\sum \iota \eta)^2 + D\sum \iota^2 \eta^2, \quad (2)$$

where ι and η are the direction cosines of \mathbf{J} and \mathbf{H} , respectively. For the specific directions of current and magnetic field used in this work, the magnetoresistance ratio $\Delta\rho/(\rho_0 H^2)$ measures the following combinations of coefficients.

I direction	H direction	Measured coefficients
100	100	$B+C+D$
100	001	B
110	001	B
110	110	$B+\frac{1}{2}D$
110	110	$B+C+\frac{1}{2}D$

A. n -Type Samples

Although the three coefficients may be evaluated from measurements on a single specimen with the current in the $[110]$ direction, the apparatus used required

remounting (and therefore resurfacing) of the crystal to change the magnetic field from the $[001]$ to the $[110]$ direction. Since n -type crystals of uniform purity and quality were available, it was usually more convenient to use both the $[100]$ and the $[110]$ current directions in obtaining the coefficients. Magnetoresistance measurements were made on seven oriented n -type samples. The experimental results for two samples, $N5$ $[110]$ ¹⁸ and $N9$ $[100]$, will be discussed in detail. However, these results are typical of all of the n -type samples investigated.

The variation of the magnetoresistance ratio with the angle between the current and the magnetic field directions for sample $N5$ is shown in Fig. 3. The expected sine-squared dependence of the magnetoresistance on the angle between \mathbf{I} and \mathbf{H} is verified. The dependence of the magnetoresistance effect on the magnetic field strength for samples $N5$ and $N9$ at 77° , 195° , and 273°K is shown in Fig. 4. Certain general features common to all curves obtained at a single temperature will now be discussed. At 77°K the transverse magnetoresistance curve only approaches a slope of 2 at the lowest fields. At the highest fields $\Delta\rho/\rho_0$ approaches a linear magnetic field dependence. The longitudinal magnetoresistance is always at least a factor of 10 smaller than the transverse effect. Only the order of magnitude of the longitudinal effect is significant, however, since the true effect is small and the measured values probably reflect more the changing of the pattern of current flow with magnetic field strength than the true longitudinal magnetoresistance. The negative longitudinal magnetoresistance values are undoubtedly a result of this phenomenon since they were not reproducible when the sample was remounted. The reliability of the transverse magnetoresistance values at 77°K is established by the good agreement of the results obtained on samples having width and thickness variations as large as a factor of two. At 195°K the transverse magnetoresistance follows

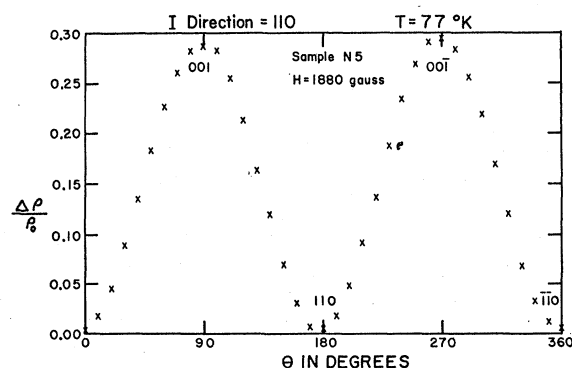


FIG. 3. Dependence of the magnetoresistance ratio upon the angle between the current and the magnetic field for the n -type specimen $N5$.

¹⁸ The numbers in the brackets refer to the crystallographic direction of the longest dimension of the sample, i.e., the direction of the current.

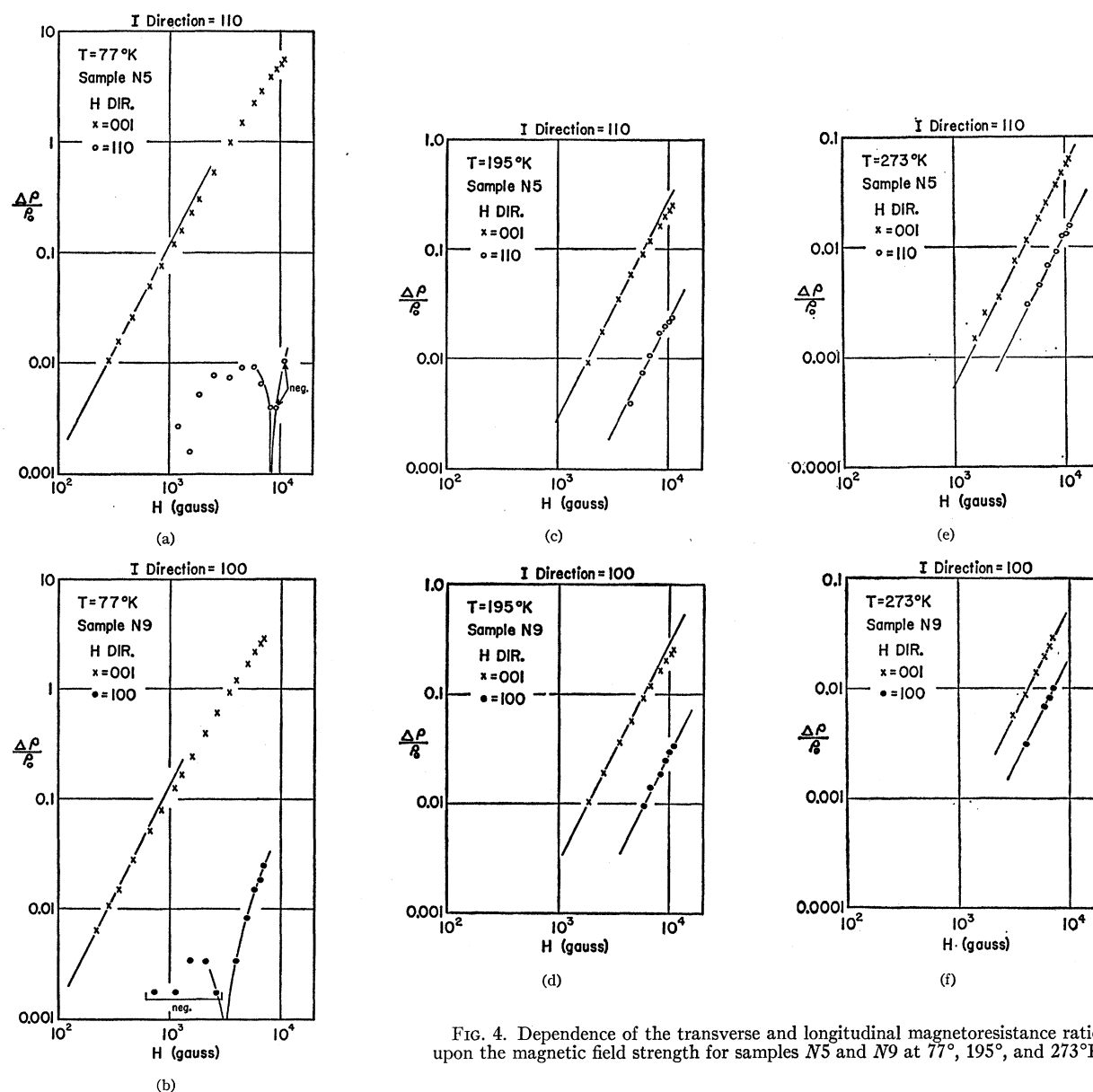


FIG. 4. Dependence of the transverse and longitudinal magnetoresistance ratios upon the magnetic field strength for samples *N5* and *N9* at 77°, 195°, and 273°K.

an H^2 dependence for fields below 3 kgauss, while the longitudinal effect has an H^2 dependence over the entire range of fields investigated. The longitudinal effect is small compared to the transverse effect, but has a definite measurable value which depends upon crystal orientation. At 273°K both the longitudinal and the transverse magnetoresistance have an H^2 dependence for all magnetic fields investigated. Although the longitudinal effect is smaller than the transverse effect, it has an appreciable value, indicating a significant anisotropy. Here again the magnitude of the longitudinal effect varies with crystal orientation. Although the longitudinal curve in Fig. 4(f) contains only four points, all crystals of the same orientation confirm this result.

To evaluate the low-field magnetoresistance coefficients, it is necessary to determine $\Delta\rho/(\rho_0 H^2)$ as H approaches zero. At 273 and 195°K the magnetoresistance in the low-field region follows an H^2 dependence and hence $\Delta\rho/(\rho_0 H^2)$ is, within the experimental error, a constant. At 77°K neither the longitudinal nor transverse effect has reached the H^2 region even at fields as low as 250 gauss, as may be seen from replots of the data such as those shown in Fig. 5 for the transverse effect. However, approximate zero-field values of the transverse effect may be extrapolated from these curves. For the longitudinal effect, a replot of the data is not useful due to the randomness of the experimental points. The experimental results of the magnetoresistance measurements for all of the n -type crystals are

TABLE II. Results of the magnetoresistance measurements on *n*-type samples expressed in terms of combinations of the phenomenological coefficients. All magnetoresistance coefficients have units of gauss⁻²×10⁻⁹.

Sample	77°K				195°K			273°K			
	<i>B</i>	<i>B</i> +½ <i>D</i>	<i>B</i> + <i>C</i> + <i>D</i>	<i>B</i> + <i>C</i> +½ <i>D</i>	<i>B</i>	<i>B</i> + <i>C</i> + <i>D</i>	<i>B</i> + <i>C</i> +½ <i>D</i>	<i>B</i>	<i>B</i> +½ <i>D</i>	<i>B</i> + <i>C</i> + <i>D</i>	<i>B</i> + <i>C</i> +½ <i>D</i>
N3 [100]	150		15					0.550		0.190	
N4 [100]	110		10					0.510		0.192	
N9 [100]	130		≈ -1		2.90	0.29		0.570		0.220	
N5 [110]	130			≈ 2	2.77		0.22	0.530			0.128
N6 [110]	163			≈ 2				0.540			0.135
N7 [110]	110			≈ 2				0.510			0.123
N8 [110]	66	70		≈ 3				0.583	0.625		0.137

summarized in Table II. In view of the difficulty in obtaining reproducible zero-field values of the longitudinal effect at 77°K, the tabulated values for it must be considered only order-of-magnitude estimates. Since, however, the quantities $B+C+\frac{1}{2}D$ and $B+C+D$ are, in every case, only a few percent of B , it is concluded from these estimates that there is no measurable anisotropy at 77°K. At the higher temperatures where a measurable anisotropy exists, the individual coefficients are evaluated from the data of Table II by combining the results from two or more samples of different orientation. At 273°K, data on seven samples are available and one can use the average values of B , $B+C+D$, and $B+C+\frac{1}{2}D$ from all crystals to calculate average values of B , C , and D , or one can choose two well matched crystals such as *N4* and *N7* and combine the results to obtain the coefficients. The results of both calculations are shown in Table III together with the

coefficients at 195°K which were evaluated from *N5* and *N9* data.

B. *p*-Type Sample

The phenomenological coefficients for *p*-type gray tin have been evaluated by using a procedure similar to that for *n*-type material. However, in *p*-type gray tin the impurity concentration varies between crystals. Consequently, it was necessary to use a sample having its long dimension in the [110] direction to permit the evaluation of all of the coefficients from the one crystal. The magnetoresistance measurements were made only at 77°K since moderately doped material becomes *n* type at higher temperatures. More heavily doped material remains *p*-type at higher temperatures, but the scattering due to ionized impurities is also more dominant at the higher temperatures. Until more pure tin is available, it is not possible to study the magnetoresistance of *p*-type material in a region where lattice-scattering predominates.

Magnetoresistance measurements have been made on one *p*-type crystal, sample *P1* [110]. The variation of the magnetoresistance ratio with the angle between

TABLE III. Phenomenological magnetoresistance coefficients of *n*-type gray tin. All magnetoresistance coefficients have units of gauss⁻²×10⁻⁹.

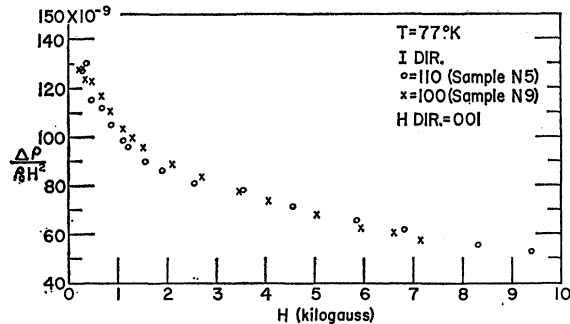
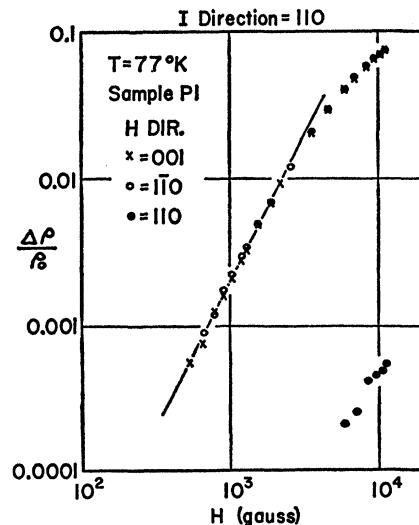
Coefficient	77°K		195°K		273°K
<i>B</i>	123 ^a	110 ^b	2.83 ^c	0.542 ^a	0.510 ^b
<i>C</i>	-123 ^d		-2.68 ^c	-0.481 ^a	-0.456 ^b
<i>D</i>	≈ 0 ^d		0.134 ^c	0.140 ^a	0.138 ^b

^a Evaluated using average values of B , $B+C+D$, and $B+C+\frac{1}{2}D$ for all *n*-type samples.

^b Evaluated using data for samples *N4* and *N7* only.

^c Evaluated using data for samples *N5* and *N9*.

^d Evaluated assuming that the measured values of $B+C+D$ and $B+C+\frac{1}{2}D$ are negligible compared to B .

FIG. 5. Magnetic field dependence of the reduced magnetoresistance ratio, $\Delta\rho/(\rho_0 H^2)$, for the *n*-type specimens at 77°K.FIG. 6. Dependence of the transverse and longitudinal magnetoresistance ratios upon the magnetic field strength for sample *P1* at 77°K.

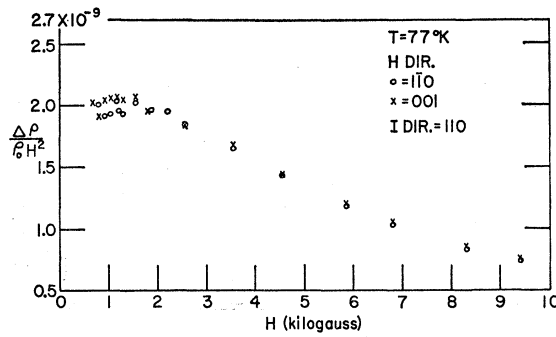


FIG. 7. Magnetic field dependence of the reduced magnetoresistance ratio, $\Delta\rho/(\rho_0 H^2)$, for the p -type specimen P1 at 77°K.

I and **H** was checked and again the sine-squared dependence was verified. The dependence of the magnetoresistance effect on the magnetic field strength is shown in Fig. 6. The transverse effect has an H^2 dependence in fields below approximately 2000 gauss as is verified by the replot of the data in Fig. 7. The extrapolated zero-field value of $\Delta\rho/(\rho_0 H^2)$ is 2×10^{-9} gauss $^{-2}$. The longitudinal effect did not reproduce exactly when the crystal was remounted, but the order of magnitude remained the same and the values were always of the order of one percent of the transverse effect. Therefore, as in the case of the n -type material, it is concluded that p -type gray tin shows no measurable anisotropy at 77°K.

V. DISCUSSION

At 77°K neither p - nor n -type gray tin shows a measurable anisotropy in the magnetoresistance. At 273°K, the low-field coefficients for the n -type material satisfy approximately the symmetry condition¹⁰ $B = -C$ and $D > 0$ indicating ellipsoidal energy surfaces oriented along the $[111]$ directions. At 195°K, the low-field coefficients satisfy about equally well the symmetry conditions for $[110]$ (i.e., $B + C = D$ and $D > 0$) or $[111]$ oriented ellipsoids. When the value of the coefficient D is small compared to the coefficients B and C , it is difficult to distinguish between these two cases. However, since the $[111]$ symmetry condition applies at 273°K where D has its largest relative value, it is assumed that this is also true at 195°K.

For the case of $[111]$ oriented ellipsoids, the relation between the magnetoresistance coefficients and the anisotropy parameter K may be written as¹²

$$B + C + D/B + (R_0\sigma_0)^2 = 2(K-1)^2/(2K+1)(K+2), \quad (3)$$

where $K = K_m/K_r$, $K_m = m_l/m_t$, $K_r = \tau_l/\tau_t$, and $R_0\sigma_0$ is the majority carrier mobility. The evaluation of K in the present case is complicated by the fact that the anisotropy is observed only in the intrinsic region. Since, however, a mobility ratio greater than unity is indicated by the p -type Hall and conductivity data, we shall assume that this is true also for n -type material and substitute electron mobility for $R_0\sigma_0$, thereby attributing the observed anisotropy to the conduction

TABLE IV. Values of the anisotropy parameter K .

	T (°K)	K
n -type	77°	≈ 1
	195°	1.6
	273°	2.3
p -type	77°	≈ 1

band. To estimate K the previously determined¹⁷ electron mobilities of 3000 and 4850 cm 2 /v-sec at 273°K and 195°K, respectively, are used in Eq. (3). The resulting estimated values of K shown in Table IV should be considered lower limits since the electron current anisotropy is reduced by the hole current which is assumed to be isotropic and is not negligible.

The interpretation of the magnetoresistance results depends not only on the energy band structure, but also on the scattering mechanism. In gray tin of the purity used in this work, the scattering by ionized impurities is dominant at 77°K and scattering by lattice vibrations is dominant at 273°K. In germanium it has been shown¹⁹ that $K_r \approx 1$ for lattice scattering, while ionized impurity scattering is anisotropic with K_r values greater than unity. If the relaxation time behavior for gray tin is similar, the decrease in the measured mobility anisotropy with decreasing temperature could be the result of the greater anisotropic scattering from ionized impurities at the lower temperatures. Assuming this to be the case, the value of K at 273°K is a lower limit for the effective-mass anisotropy in the conduction band.

A second possible explanation of the temperature-dependent anisotropy can be seen from Herman's predictions on the energy band structure of gray tin.²⁰ He indicates the lowest lying minimum in the conduction band is a spherically symmetric band located at $\mathbf{k} = 0$. A second set of minima slightly higher in energy are located along the $[111]$ reciprocal axes. The increase in the thermal energy gap of gray tin with increasing impurity concentration²¹ indicates the density of states near the bottom of the spherically symmetric band is small, and hence it becomes degenerate at moderate carrier densities and the energy levels are filled well above the bottom of the conduction band. Thus the conduction electrons occupy states in the spherically symmetric band at low temperatures and at higher temperatures, where gray tin is intrinsic, an appreciable number of electrons are excited into the second anisotropic band. Since the fraction of the total current carried by the electrons with an anisotropic effective mass is small, the mass anisotropy in the $[111]$ minima must be large to produce the measured anisotropy in the mobility. On the basis of the present measurements, it is not possible to determine which, if either, of these models is the correct explanation of the temperature-dependent anisotropy.

¹⁹ R. A. Laff and H. Y. Fan, Phys. Rev. **112**, 317 (1958).

²⁰ F. Herman, J. Electronics **1**, 103 (1955).

²¹ A. W. Ewald and E. E. Kohnke, Phys. Rev. **97**, 607 (1955).